Progress In Electromagnetics Research, PIER 99, 261–272, 2009

CONDUCTIVE MEDIUM MODELING WITH AN AUGMENTED GIBC FORMULATION

Z.-G. Qian, M. S. Tong, and W. C. Chew

Department of Electrical and Computer Engineering
University of Illinois at Urbana-Champaign
1406 W Green St., Urbana, IL 61801, USA

Abstract—This paper describes an augmented generalized impedance boundary condition (AGIBC) formulation for accurate and efficient modeling of conductive media. It is a surface integral equation method, so that it uses a smaller number of unknowns. The underlying GIBC provides a rigorous way to account for the skin effect. Combining with the novel augmentation technique, the AGIBC formulation works stably in the low-frequency regime. No loop-tree search is required. The formulation also allows for its easy incorporation of fast algorithms to enable the solving of large problems with many unknowns. Numerical examples are presented to validate the formulation.

1. INTRODUCTION

Conductive media are widely encountered in real-world problems, such as high-speed interconnect design, antenna radiation, radar scattering, well-logging and subsurface detection. The difference of scales between the outer propagation physics and the inner diffusion physics causes difficulties for numerical methods. The small skin depth usually causes a prohibitively large number of unknowns for those methods requiring a volumetric discretization of the conductive medium. A popular alternative uses an impedance boundary condition (IBC) [1], which approximates the effect of the conductive medium without discretizing it. However, these IBCs are usually derived from a simplified 2-D analysis. They are by no means rigorous and may cause large errors for strongly coupled structures.

Surface integral equations (SIEs) can model conductive medium rigorously by treating it as a general complex medium and formulating

Corresponding author: W. C. Chew (w-chew@uiuc.edu).

integral equations for it. The effect of the conductive medium is accounted by the lossy Green's function. To this end, a generalized impedance boundary condition (GIBC) has been introduced in the literature [2]. Numerical examples demonstrate that GIBC can model conductors with good accuracy as well as high efficiency. It also elucidates the relationship between the rigorous model and the approximate IBC model with a two-step approximation.

Because of the electric field integral equation (EFIE) operator, GIBC has a low-frequency breakdown problem. Previously, a loop-tree decomposition is used as a remedy [2]. However, the search for loop basis is very tricky for complex structures. Recently we have developed an augmentation technique to remedy the low-frequency breakdown of the EFIE operator [3, 4]. Therefore, we combine GIBC with the novel augmentation technique to formulate an augmented GIBC (AGIBC) method. The AGIBC method does not need to search for the loop basis. It also inherits the established solution scheme of A-EFIE.

In this paper, we briefly review the GIBC formulation at first, then the AGIBC method is discussed in details. Finally, several numerical examples are presented to validate the proposed formulation.

2. GIBC FORMULATION

SIEs only consider the surface of an object. For a general multiple-object problem, the notations of the surfaces and regions are illustrated in Fig. 1. Assuming that each surface contains a homogeneous volume, all N surfaces are numbered from S_1 to S_N, and the volume enclosed by S_ν is indexed as V_ν. The outermost region is named as V_0. In region V_ν, the permittivity and permeability are ϵ_ν and μ_ν, respectively. The wave impedance is thus $\eta_\nu = \sqrt{\mu_\nu \epsilon_\nu^{-1}}$. Here, the index ν runs from 0 to N. The wave number in free space is $k = \omega\sqrt{\mu\epsilon}$, and the wave number in region ν is $k_\nu = \omega\sqrt{\mu_\nu\epsilon_\nu}$.

On surface S_ν, the electric current is $\mathbf{J}_\nu$, and magnetic current is $\mathbf{M}_\nu$. In region V_ν, the incident electric field is $\mathbf{E}^\nu_{inc}$, and the incident

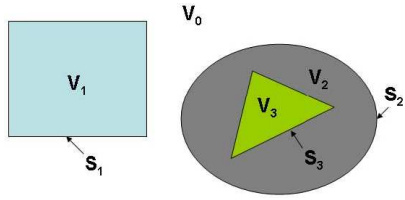

Figure 1. An illustration of the multi-object problem.

magnetic field is $\mathbf{H}^{\nu}_{inc}$. In the following formulations, the magnetic current and the incident electric field are normalized by the free space impedance η as $\widetilde{\mathbf{E}}^{\nu}_{inc} = \eta^{-1}\mathbf{E}^{\nu}_{inc}$, and $\widetilde{\mathbf{M}}_{\nu} = \eta^{-1}\mathbf{M}_{\nu}$.

In general, the EFIE and MFIE operators in region ν are written as

$$\widetilde{\mathcal{L}}^{\nu}_{pq} = i\omega\eta^{-1}\mu_{\nu}\left(\bar{\mathbf{I}} + \frac{\nabla\nabla}{k^2_{\nu}}\right) g_{\nu}\left(\mathbf{r}_p, \mathbf{r}'_q\right) \tag{1}$$

$$\mathcal{K}^{\nu}_{pq} = \nabla g_{\nu}\left(\mathbf{r}_p, \mathbf{r}'_q\right) \times \bar{\mathbf{I}} \tag{2}$$

where p and q refer to testing surface and source surface, respectively. The scalar Green's function is defined as

$$g_{\nu}\left(\mathbf{r}, \mathbf{r}'\right) = \frac{\exp\left(ik_{\nu}|\mathbf{r} - \mathbf{r}'|\right)}{4\pi|\mathbf{r} - \mathbf{r}'|} \tag{3}$$

and the EFIE operator is normalized by η.

For a single penetrable object, EFIE in the outer region and MFIE in the inner region are written as

$$\widetilde{\mathcal{L}}^{0}_{11}\mathbf{J}_1 + \mathcal{K}^{0}_{11}\widetilde{\mathbf{M}}_1 = -\widetilde{\mathbf{E}}^{0}_{inc} \tag{4}$$

$$\mathcal{K}^{1}_{11}\mathbf{J}_1 - \tau_1\widetilde{\mathcal{L}}^{1}_{11}\widetilde{\mathbf{M}}_1 = \mathbf{0} \tag{5}$$

where $\tau_{\nu} = \eta^2\eta_{\nu}^{-2}$ and integrations are implied over repeated variable. Combining them, we get the GIBC formulation [2]. Both the electric current and magnetic current are expanded with the RWG basis functions [8],

$$\mathbf{J}_1 = \sum_n j_{1n}\mathbf{\Lambda}_n, \qquad \widetilde{\mathbf{M}}_1 = \sum_n m_{1n}\mathbf{\Lambda}_n \tag{6}$$

where j_{1n} is the nth element of the expansion coefficient vector $\mathbf{j}_1$, and m_{1n} is the nth element of the expansion coefficient vector $\mathbf{m}_1$. With the Galerkin testing, the integral equations can be converted into a matrix form as

$$\begin{bmatrix} \bar{\mathbf{L}}^{0}_{11} & \bar{\mathbf{K}}^{0}_{11} - \frac{1}{2}\bar{\mathbf{X}}_1 \\ \bar{\mathbf{K}}^{1}_{11} + \frac{1}{2}\bar{\mathbf{X}}_1 & -\tau_1\bar{\mathbf{L}}^{1}_{11} \end{bmatrix} \cdot \begin{bmatrix} \mathbf{j}_1 \\ \mathbf{m}_1 \end{bmatrix} = \begin{bmatrix} \mathbf{b}^{0}_{E1} \\ \mathbf{0} \end{bmatrix} \tag{7}$$

The expressions for the sub-matrices and vectors are listed in the Appendix. Invoking the Schur complement and defining the impedance matrix as

$$\bar{\mathbf{Z}}_1 = \left(\bar{\mathbf{L}}^{1}_{11}\right)^{-1} \cdot \left(\bar{\mathbf{K}}^{1}_{11} + \frac{1}{2}\bar{\mathbf{X}}_1\right) \tag{8}$$

the equation system is reduced to a single equation

$$\left[\bar{\mathbf{L}}^{0}_{11} + \tau_1^{-1}\left(\bar{\mathbf{K}}^{0}_{11} - \frac{1}{2}\bar{\mathbf{X}}_1\right) \cdot \bar{\mathbf{Z}}_1\right] \cdot \mathbf{j}_1 = \mathbf{b}^{0}_{E1} \tag{9}$$

with electric current as the unknown. The magnetic current is then determined by

$$\mathbf{m}_1 = \tau_1^{-1} \bar{\mathbf{Z}}_1 \cdot \mathbf{j}_1 \tag{10}$$

The final equation in (9) is the GIBC formulation. It is also named as the GIBC-e form because the unknown vector is the electric current. The implementation details and solution method are presented in [2] and are omitted here. It is also straightforward to generalize the formulation for multi-conductor problems. For simplicity of derivation, we only show the single conductor case.

3. AGIBC FORMULATION

3.1. Augmented Formulation

The EFIE operator in GIBC has the low-frequency breakdown problem, so that the GIBC matrix is singular at low frequencies. Traditional remedy is to use the loop-tree decomposition. However, the search for loop basis is very tricky for real-world complex structures.

It has been shown in [4] that the augmentation technique can remedy the low-frequency breakdown. The EFIE operator comprises contributions of both the vector potential and the scalar potential. The two can be separated by including the charge as extra unknown. With the current continuity condition, the expanded system, named A-EFIE, is free of low-frequency breakdown. Similar to AEFIE, GIBC-e in (9) can be augmented to obtain the AGIBC-e form:

$$\begin{bmatrix} ik\bar{\mathbf{V}}_{11}^0 + \tau_1^{-1}\left(\bar{\mathbf{K}}_{11}^0 - \frac{1}{2}\bar{\mathbf{X}}_1\right)\cdot\bar{\mathbf{Z}}_1 & \bar{\mathbf{D}}_1^T\bar{\mathbf{P}}_{11}^0\bar{\mathbf{B}}_1 \\ \bar{\mathbf{F}}_1\bar{\mathbf{D}}_1 & -ik\bar{\mathbf{I}} \end{bmatrix} \cdot \begin{bmatrix} \mathbf{j}_1 \\ c\boldsymbol{\rho}_{r1}^e \end{bmatrix} = \begin{bmatrix} \mathbf{b}_{E1}^0 \\ \mathbf{0} \end{bmatrix} \tag{11}$$

where the EFIE operator $\bar{\mathbf{L}}_{11}^0$ is augmented. Matrices $\bar{\mathbf{V}}_{11}^0$ and $\bar{\mathbf{P}}_{11}^0$ represent the vector potential and the scalar potential, respectively. The detailed expressions of them are listed in the Appendix. Vector $\boldsymbol{\rho}_{r1}^e$ is the reduced charge vector due to the enforcement of charge neutrality. Take a single connected object as an example. The charge neutrality states that the summation of all the charge unknowns is zero. Thus, one degree of freedom can be removed to form the reduced charge vector. Backward matrix $\bar{\mathbf{B}}_1$ and forward matrix $\bar{\mathbf{F}}_1$ project the original and reduced charge vectors back and forth. If the last element gets removed, the backward matrix is a unit matrix with an additional row of all negative ones, and the forward matrix is a unit matrix without the last column. The constant c is the speed of light in free space. From this equation, we can solve for $\mathbf{j}_1$ and $\boldsymbol{\rho}_{r1}^e$, and then obtain $\mathbf{m}_1$ by (10). Notice that the frequency scaling in AGIBC is different from that in A-EFIE. That is because the loss dominates the physics of AGIBC in the low-frequency regime.

3.2. Dual Formulation

The aforementioned GIBC-e formulation in Equation (7) reduces to a modified EFIE in Equation (9) with electric current as the unknown. A dual form, the GIBC-h form, can be alternatively derived by combining MFIE in the outer region and EFIE in the inner region.

$$\begin{bmatrix} \tau_0\widetilde{\mathcal{L}}_{11}^0 & -\mathcal{K}_{11}^0 \\ \mathcal{K}_{11}^1 & \widetilde{\mathcal{L}}_{11}^1 \end{bmatrix} \cdot \begin{bmatrix} \widetilde{\mathbf{M}}_1 \\ \mathbf{J}_1 \end{bmatrix} = \begin{bmatrix} -\widetilde{\mathbf{H}}_{inc}^0 \\ \mathbf{0} \end{bmatrix} \tag{12}$$

Converted into matrix form with MoM, the GIBC-h form is written as

$$\left[\tau_0\bar{\mathbf{L}}_{11}^0 - \left(\bar{\mathbf{K}}_{11}^0 - \frac{1}{2}\bar{\mathbf{X}}_1\right)\cdot\bar{\mathbf{Z}}_1\right]\cdot\mathbf{m}_1 = \mathbf{b}_{H1}^0 \tag{13}$$

with magnetic current as the unknown. The electric current can be calculated by

$$\mathbf{j}_1 = -\bar{\mathbf{Z}}_1\cdot\mathbf{m}_1 \tag{14}$$

The AGIBC-h form is obtained with the augmentation technique

$$\begin{bmatrix} ik\tau_0\bar{\mathbf{V}}_{11}^0 - \left(\bar{\mathbf{K}}_{11}^0 - \frac{1}{2}\bar{\mathbf{X}}_1\right)\cdot\bar{\mathbf{Z}}_1 & \tau_0\bar{\mathbf{D}}_1^T\bar{\mathbf{P}}_{11}^0\bar{\mathbf{B}}_1 \\ \bar{\mathbf{F}}_1\bar{\mathbf{D}}_1 & -ik\bar{\mathbf{I}} \end{bmatrix}\cdot\begin{bmatrix} \mathbf{m}_1 \\ c\boldsymbol{\rho}_{r1}^m \end{bmatrix} = \begin{bmatrix} \mathbf{b}_{H1}^0 \\ \mathbf{0} \end{bmatrix} \tag{15}$$

It can also be derived using duality. From this equation, we can solve for $\mathbf{m}_1$ and $\boldsymbol{\rho}_{r1}^m$, and then obtain $\mathbf{j}_1$ by (14).

It is noted that AGIBC-e asks for electric field excitation, while AGIBC-h needs magnetic field incidence. Readers are referred to paper [4] for efficient solution scheme of the matrix equation.

3.3. Power Calculation

The matrix equation in (11) or (15) can be solved by either direct solvers or iterative solvers. Then, various results can be retrieved from the known current distributions. Here, we derive a succinct expression to calculate the time average power dissipated into the conductor. Assume that the conductor is enclosed by surface S_1, the time average power is expressed using Poynting's vector:

$$P_{av} = \frac{1}{2}\mathrm{Re}\left[\oint_{S_1}\mathbf{E}_1\times\mathbf{H}_1^*\cdot(-\hat{n}_1)\,\mathrm{d}S\right] \tag{16}$$

The integral kernel yields

$$\begin{aligned} \mathbf{E}_1\times\mathbf{H}_1^*\cdot\hat{n}_1 &= (\hat{n}_1\times\mathbf{M}_1)\times(-\hat{n}_1\times\mathbf{J}_1^*)\cdot(-\hat{n}_1) \\ &= (\hat{n}_1\times\mathbf{M}_1)\cdot(-\hat{n}_1\times\hat{n}_1\times\mathbf{J}_1^*) \\ &= \mathbf{J}_1^*\cdot(\hat{n}_1\times\mathbf{M}_1) \end{aligned} \tag{17}$$

Substituting the expansion of the currents in (6), and then performing the integration, the time-average power can be simply written as

$$P_{av} = \frac{1}{2}\mathrm{Re}\left[\mathbf{j}_1^H \cdot \bar{\mathbf{X}}_1 \cdot \mathbf{m}_1\right] \tag{18}$$

It involves one matrix-vector product and one vector inner product. Notice that matrix $\bar{\mathbf{X}}_1$ is highly sparse, as shown in the Appendix.

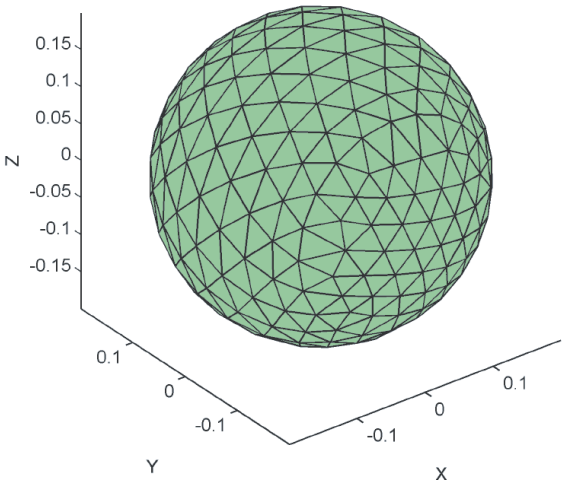

Figure 2. The mesh of a sphere.

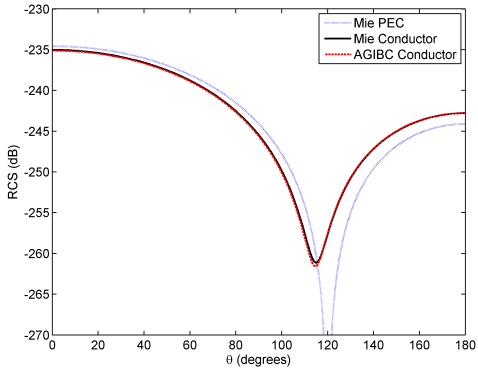

Figure 3. The bistatic RCS of a conductive sphere at 10 MHz. The sphere is located at the origin with a radius of 0.2 mm and a conductivity of 5.8×10^7 S/m.

4. NUMERICAL EXAMPLES

Numerical examples are presented in this section to validate the AGIBC method. AGIBC-e form in Equation (11) is used. The first example is the plane wave scattering of a conductive sphere with radius 0.2 mm and conductivity 5.8×10^7 S/m. The surface of the sphere is discretized into 1,568 triangular patches as shown in Fig. 2, so there are 2,352 inner edges for surface integral equation methods. The x polarized plane-wave impinges onto the sphere from the $+z$ direction at 10 MHz. For such a low-frequency scattering problem, GIBC fails to deliver correct solutions. However, the new AGIBC formulation remedies the low-frequency breakdown without using the loop-tree decomposition. The result agrees well with the Mie series solution as shown in Fig. 2. The lossless case is also included to demonstrate the effect of conductor loss.

Then, we calculate the near field of a conductive sphere with a magnetic dipole excitation. The sphere is located at the origin with a radius of 5 mm. The conductor has a relative permeability of 20 and a conductivity of 2×10^6 S/m. The surrounding medium has a dielectric constant of 3.0. A z-polarized magnetic dipole with unit dipole moment is placed on the z axis at $z = 50$ mm. The scattered electric field, shown in Fig. 3, is calculated along the line $x \in [-10, 10]$ mm, $y = 0$ mm, and $z = 10$ mm. It agrees well with the Mie series solution.

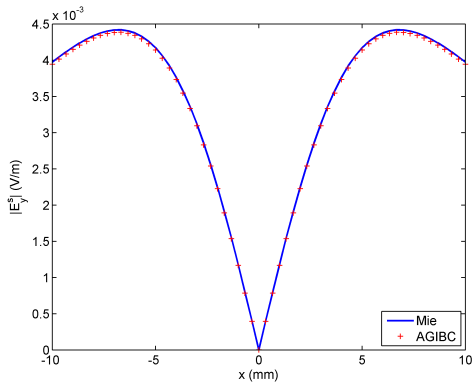

Figure 4. Scattering electric field at $x \in [-10, 10]$ mm, $y = 0$ mm, and $z = 10$ mm. The sphere is located at the origin with radius of 5 mm and conductivity of 2×10^6 S/m. A z-polarized magnetic dipole with unit dipole moment is placed on the z axis at $z = 50$ mm. The frequency is 1 kHz.

The next example is a copper rectangular loop, which is shown in Fig. 5. It has a typical scale of on-chip interconnects. The length and width are 1,984 μm and 122 μm, respectively. The cross section is 4 μm by 4 μm, and the conductivity of copper is set to be 5.8×10^7 S/m. A single delta-gap voltage source is assigned in the middle of a short side. The triangular mesh contains 448 triangle patches and 672 inner edges. To validate the AGIBC formulation, the input admittance is extracted over a broad frequency band from 0.01 GHz to 10 GHz. Correspondingly, the skin depth decreases from 20.9 μm to 0.661 μm. Good agreement between AGIBC and FastHenry [7] is shown in Fig. 4.

The last example is a rectangular conductive plate shown in Fig. 7. It is 0.5 mm by 0.5 mm with a thickness of 0.02 mm. A plane wave impinges from the $-x$ direction with $E_y = 1.0$ V/m at 0.1 GHz. It is a low-frequency problem in the magnetic diffusion regime. The time-average dissipated power is plotted in Fig. 5 for a wide range of conductivities. Notice that Krakowski's formula [5] was derived based on the assumption that the skin depth is much larger than the thickness of the plate. Thus, it leads to erroneous results for small skin depth [6]. The comparison shows that AGIBC agrees well with Krakowski's formula when conductivity is smaller than 2×10^4 S/m, at which the skin depth is about 20 times larger than the thickness of the plate. With the decreasing skin depth, the power dissipation increases at first and drops finally. It is consistent with the physics that the loss of a perfect electric conductor is zero. As an example, the loss is 49×10^{-15} W for conductivity of 5.8×10^6 S/m.

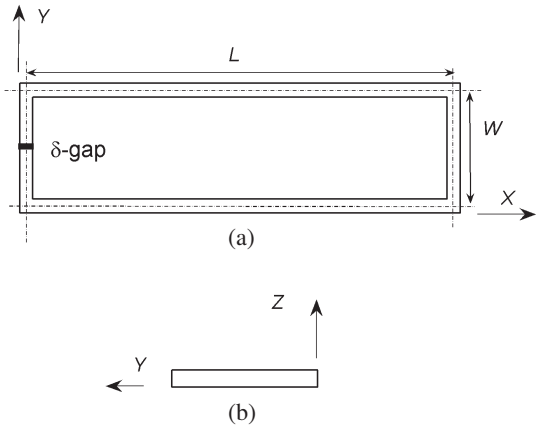

Figure 5. The geometry of a rectangular loop inductor.

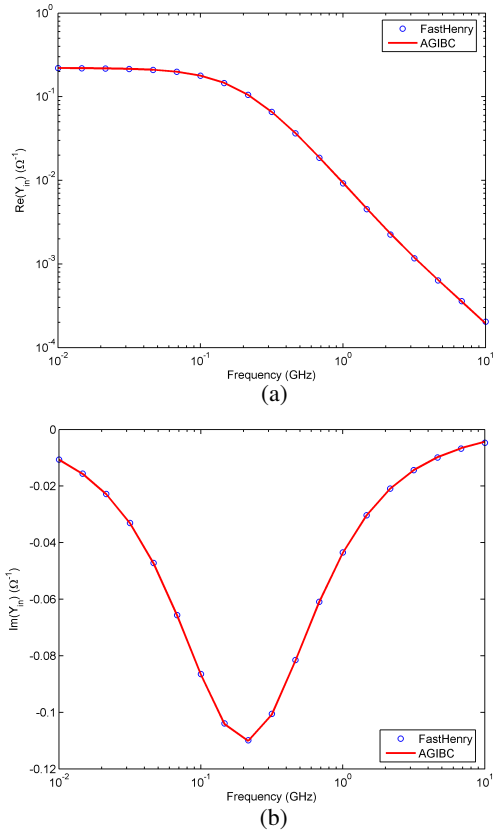

Figure 6. Real and imaginary parts of the input admittance of the copper rectangular loop.

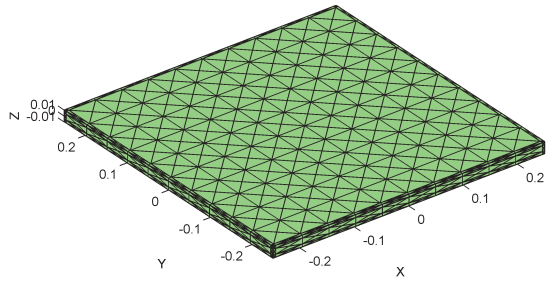

Figure 7. The mesh of a rectangular conductor plate.

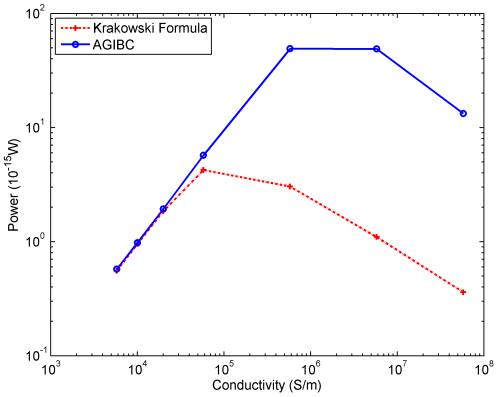

Figure 8. The dissipated power of the rectangular plate at 0.1 GHz with different conductivities.

5. CONCLUSION

AGIBC inherits the advantages of both GIBC and A-EFIE. It is a rigorous and efficient method to model conductive medium, especially when the skin depth is small. The incorporation of the augmentation technique used in A-EFIE remedies the low-frequency breakdown of GIBC. The novel method has been applied to various types of problems.

ACKNOWLEDGMENT

This research was supported by SRC 2006-KJ-1401 and AFOSR F9550-04-1-0326.

APPENDIX A. DEFINITION OF OPERATORS

The MFIE operator $\mathcal{K}_{pq}^{\nu}$ should be rewritten as $\bar{\mathcal{K}}_{pq}^{\nu} + \mathcal{R}$, if $\mathbf{r}_p$ equals $\mathbf{r}'_q$. The first term $\bar{\mathcal{K}}_{pq}^{\nu}$ takes the Cauchy principal value and the second term $\mathcal{R}$ represents the residue, which equals to $\pm\frac{1}{2}\hat{n}_p\times$ or $\pm\frac{1}{2}\hat{n}_q\times$. The sign is determined by the relationship between surface S_p and V_ν. If V_ν is the outer region of S_p, the testing is on the inner side of S_p and the residue is $-\frac{1}{2}\hat{n}_p\times$. If V_ν is the inner region of S_p, the residue is $\frac{1}{2}\hat{n}_p\times$. The relation between S_q and S_p determines the sign of the residue in terms of $\hat{n}_q$.

Denote the RWG function as $\mathbf{\Lambda}_m$, and the pulse function on a triangle patch as h_m, the matrices in EFIEs and MFIEs can be written as

$$\left[\bar{\mathbf{L}}_{pq}^{\nu}\right]_{mn} = \left\langle \mathbf{\Lambda}_m\left(\mathbf{r}_p\right), \widetilde{\mathcal{L}}_{pq}^{\nu}\mathbf{\Lambda}_n\left(\mathbf{r}'_q\right)\right\rangle \tag{A1}$$

$$\left[\bar{\mathbf{V}}_{pq}^{\nu}\right]_{mn} = \left\langle \mathbf{\Lambda}_m\left(\mathbf{r}_p\right), \frac{\mu_\nu}{\mu} g_\nu\left(\mathbf{r}_p, \mathbf{r}'_q\right)\mathbf{\Lambda}_n\left(\mathbf{r}'_q\right)\right\rangle \tag{A2}$$

$$\left[\bar{\mathbf{P}}_{pq}^{\nu}\right]_{mn} = \left\langle h_m\left(\mathbf{r}_p\right), \frac{\epsilon}{\epsilon_\nu} g_\nu\left(\mathbf{r}_p, \mathbf{r}'_q\right) h_n\left(\mathbf{r}'_q\right)\right\rangle \tag{A3}$$

$$\left[\bar{\mathbf{K}}_{pq}^{\nu}\right]_{mn} = \left\langle \mathbf{\Lambda}_m\left(\mathbf{r}_p\right), \bar{\mathcal{K}}_{pq}^{\nu}\mathbf{\Lambda}_n\left(\mathbf{r}'_q\right)\right\rangle \tag{A4}$$

$$\left[\bar{\mathbf{X}}_p\right]_{mn} = \left\langle \mathbf{\Lambda}_m\left(\mathbf{r}_p\right), \hat{n}_p \times \mathbf{\Lambda}_n\left(\mathbf{r}_p\right)\right\rangle \tag{A5}$$

The right hand side vectors are defined as

$$\left[\mathbf{b}_{Ep}^{\nu}\right]_m = \left\langle \mathbf{\Lambda}_m\left(\mathbf{r}_p\right), -\widetilde{\mathbf{E}}_{inc}^{\nu}\left(\mathbf{r}_p\right)\right\rangle \tag{A6}$$

$$\left[\mathbf{b}_{Hp}^{\nu}\right]_m = \left\langle \mathbf{\Lambda}_m\left(\mathbf{r}_p\right), -\widetilde{\mathbf{H}}_{inc}^{\nu}\left(\mathbf{r}_p\right)\right\rangle \tag{A7}$$

REFERENCES

1. Stratton, J. A., *Electromagnetic Theory*, McGraw-Hill, New York, 1941.
2. Qian, Z. G., W. C. Chew, and R. Suaya, "Generalized impedance boundary condition for conductor modeling in surface integral equation," *IEEE Trans. Microw. Theory Tech.,* Vol. 55, No. 11, 2354–2364, Nov. 2007.
3. Qian, Z. G. and W. C. Chew, "An augmented electric field integral equation for low frequency electromagnetics analysis," *IEEE International Symposium on Antennas and Propagation and USNC/URSI National Radio Science Meeting*, San Diego, Jul. 2008.
4. Qian, Z. G. and W. C. Chew, "Fast full-wave surface integral equation solver for multiscale structure modeling," *IEEE Trans. Antennas Propagat.*, Vol. 57, No. 11, 3594–3601, Nov. 2009.
5. Krakowski, M., "Eddy-current losses in thin circular and rectangular plates," *Archiv für Elekrotechnik*, Vol. 64, 307–311, 1982.
6. Prechtl, A. and H. Hass, "Some comments on the paper 'Eddy-current losses in thin circular and rectangular plates'," *Archiv für Elekrotechnik*, Vol. 66, 231–232, 1983.

7. Kamon, M., M. J. Tsuk, and J. White, "FastHenry: A multipole-accelerated 3-D inductance extraction program," *IEEE Trans. Microw. Theory Tech.*, Vol. 42, No. 9, 1750–1758, Sep. 1994.
8. Rao, S. M., D. R. Wilton, and A. W. Glisson, "Electromagnetic scattering by surface of arbitrary shape," *IEEE Trans. Antennas Propagat.*, Vol. 30, No. 3, 409–418, May 1982.